The Journal of Antibiotics (2018) 71, 273–278

www.nature.com/ja

ORIGINAL ARTICLE

Halistanol sulfates I and J, new SIRT1–3 inhibitory steroid sulfates from a marine sponge of the genus *Halichondria*

Fumiaki Nakamura[1,9], Norio Kudo[2,9], Yuki Tomachi[1], Akiko Nakata[2], Misao Takemoto[2], Akihiro Ito[3,4], Hodaka Tabei[1], Daisuke Arai[5], Nicole de Voogd[6], Minoru Yoshida[2,3,7], Yoichi Nakao[1,5] and Nobuhiro Fusetani[5,8]

Two new analogs of halistanol sulfate (1) were isolated from a marine sponge *Halichondria* sp. collected at Hachijo-jima Island. Structures of these new halistanol sulfates I (2) and J (3) were elucidated by spectral analyses. Compounds 1–3 showed inhibitory activity against SIRT 1-3 with IC_{50} ranges of 45.9–67.9, 18.9–21.1 and 21.8-37.5 μM, respectively. X-ray crystallography of the halistanol sulfate (1) and SIRT3 complex clearly indicates that 1 binds to the exosite of SIRT3 that we have discovered in this study.
The Journal of Antibiotics (2018) **71,** 273–278; doi:10.1038/ja.2017.145: published online 29 November 2017

INTRODUCTION

Sirtuins (SIRTs) are enzymes belonging to the NAD^+-dependent lysine deacetylase (KDAC) family that are highly conserved from yeast to human. There are seven isoforms of SIRTs (SIRT1–7) in mammals, and SIRT1 is mainly localized in the nucleus, whereas SIRT2 is found in the cytoplasm to control cellular cytoskeleton dynamics. SIRT3–5 are mainly localized in mitochondria and regulate mitochondrial functions.[1] SIRTs remove acetyl groups from various proteins, including histones H3 and H4, PGC-1α, p53, NF-κB, FOXO and so on, thereby regulating energy metabolism, genome stability, longevity and aging as well as age-associated pathologies.[2] SIRT2 deacetylates receptor-interacting protein 1 (RIP1) and modulates RIP1–RIP3 complex formation and tumor necrosis factor-α-stimulated necrosis. Deletion or knockdown of SIRT2 prevents formation of RIP1–RIP3 complex in mice.[3] Also, the SIRT2 inhibitor AK-7 acts as a neuroprotective agent in Huntington's disease mouse model.[4] Thus SIRTs have been one of the most promising targets of antiaging treatments.

In this study, we have attempted to discover new SIRT inhibitors from a marine sponge *Halichondria* sp. collected at Hachijo-jima Island. As a result, halistanol sulfate (**1**)[5] as well as two novel analogs were identified (Figure 1). Highly sulfated steroids such as halistanol sulfates are often found as 'HIT' in wide variety of screenings as enzyme inhibitory,[6] antimicrobial[7] or antiviral activities.[8–10] Therefore, they are often regarded as 'non-specific nuisance compounds'.[11] However, no study has shown a mechanism for enzymatic inhibitory activities of halistanol sulfate (**1**) at the molecular/atomic level. We could, for the first time, reveal the binding mode of halistanol sulfate (**1**) to SIRT3 protein at the atomic level on the basis of crystal structure study. This finding may be a cue for understanding the mechanisms of the wide variety of bioactivities of halistanol sulfate (**1**) and designing a new drug motif with sulfate groups as the pharmacophore.

RESULTS AND DISCUSSION

The frozen specimen of *Halichondria* sp. (695 g wet weight), collected by hand using SCUBA at Hachijo-jima Island, was extracted with MeOH. The combined methanolic extract was evaporated *in vacuo* and subjected to solvent partitioning and ODS flash chromatography, followed by repetitive reversed-phase HPLC. Final purification was carried out by recycling reversed-phase HPLC on C_{18} column to afford 6.6 and 3.0 mg of halistanol sulfates I (**2**) and J (**3**), respectively (9.5×10^{-3}% and 5.5×10^{-3}% yield based on wet weights). Halistanol sulfate (**1**) was also identified as the major component (301.4 mg)

[1]Department of Chemistry and Biochemistry, Graduate School of Advanced Science and Engineering, Waseda University, Tokyo, Japan; [2]Seed Compounds Exploratory Unit for Drug Discovery Platform, RIKEN Center for Sustainable Resource Science, Saitama, Japan; [3]Chemical Genomics Research Group, RIKEN Center for Sustainable Resource Science, Saitama, Japan; [4]School of Life Sciences, Tokyo University of Pharmacy and Life Sciences, Tokyo, Japan; [5]Research Institute for Science and Engineering, Waseda University, Tokyo, Japan; [6]Naturalis Biodiversity Center, Leiden, The Netherlands; [7]Department of Biotechnology, Graduate School of Agricultural Life Sciences, The University of Tokyo, Tokyo, Japan and [8]Fisheries and Oceans Hakodate, Hakodate, Japan
[9]These authors contributed equally to this work.
Correspondence: Dr M Yoshida, RIKEN, Chemical Genetics Laboratory, 2-1 Hirosawa, Wako, Saitama 351-0198, Japan.
E-mail: yoshidam@riken.jp
or Professor Y Nakao, Department of Chemistry and Biochemistry, Graduate School of Advanced Science and Engineering, Waseda University, 3-4-1 Okubo, Shinjuku-ku, Tokyo 169-8555, Japan.
E-mail: ayocha@waseda.jp
Received 8 August 2017; revised 14 October 2017; accepted 17 October 2017: published online 29 November 2017

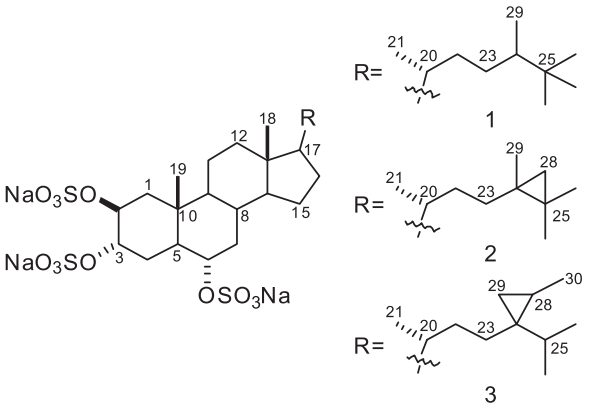

Figure 1 Structure of halistanol sulfate (**1**), halistanol sulfates I (**2**) and J (**3**).

based on the HRESIMS (*m/z* 731.2194 [M-Na]$^-$, calcd for $C_{29}H_{49}Na_2O_{12}S_3$ *m/z* 731.2187) and NMR data (see Table 1).

Halistanol sulfate I (**2**) had a molecular formula of $C_{29}H_{47}Na_3O_{12}S_3$, which was determined by the negative mode HRESIMS analysis (*m/z* 729.2027 [M-Na]$^-$, calcd for $C_{29}H_{47}Na_2O_{12}S_3$ *m/z* 729.2031). The ESIMS showed sequencial ion peaks at *m/z* 729.2 [M-Na]$^-$, 609.3 [729.2-$NaSO_4H$]$^-$ and 489.3 [609.3-$NaSO_3H$]$^-$, indicating that **2** have three sulfate groups in the molecule. IR absorption at 1248 and 1220 cm^{-1} supported the presence of the sulfate groups. ^{1}H and ^{13}C NMR spectra of **2** (Table 1) indicated the similarity between two structural features of **1** and **2**; that is, two singlet methyl protons at C-18 and 19 (δ_H 0.69 and 1.06, respectively) and three oxymethine protons at C-2, C-3, and C-6 (δ_H 4.80/4.82, 4.75/4.74 and 4.19/4.15, respectively, for **1**/**2**). Based on the COSY and HMQC correlations, as well as HMBC cross peaks from the H_3-18, H_3-19, and H_3-21, the same steroidal core (C-1 to C-22) as **1** was

Table 1 NMR spectral data for halistanol sulfate (1) and halistanol sulfates I (2) and J (3) in CD_3OD (400 MHz)

	*Halistanol sulfate (**1**)*		*Halistanol sulfate I (**2**)*		*Halistanol sulfate J (**3**)*	
Position	δ_C	δ_H *mult. (J in Hz)*	δ_C	δ_H *mult. (J in Hz)*	δ_C	δ_H *mult. (J in Hz)*
1	39.4	2.09 brd (14.2) 1.46 dd (14.2, 3.5)	39.4	2.10 brd (14.3) 1.48 dd (14.3, 3.8)	39.3	2.10 brd (14.3) 1.47 dd (14.3, 3.5)
2	75.7	4.80 m	75.7	4.82 m	75.7	4.83 m
3	75.7	4.75 m	75.7	4.74 m	75.7	4.74 m
4	25.3	2.29 brd (14.7) 1.80 ddd (14.7, 12.8, 2.3)	25.3	2.29 brd (14.5) 1.80 dt (14.5, 2.5)	25.3	2.29 brd (14.7) 1.80 ddd (14.7, 12.8, 2.5)
5	45.5	1.65 ddd (12.8, 10.7, 2.4)	45.5	1.65 ddd (12.4, 10.4, 2.5)	45.5	1.65 ddd (12.8, 11.1, 2.5)
6	78.9	4.19 td (10.7, 4.5)	78.9	4.15 td (10.7, 4.5)	78.9	4.19 td (11.1, 4.5)
7	40.2	2.37 ddd (12.5, 4.5, 4.1) 1.03 m	40.2	2.37 dt (12.0, 3.9) 1.02 m	40.2	2.37 dt (12.4, 4.0) 1.03 m
8	35.3	1.54 m	35.3	1.53 m	35.3	1.53 m
9	56.0	0.75 m	56.0	0.76 m	56.0	0.76 m
10	37.8		37.8		37.8	
11	22.0	1.54 m, 1.34 m	22.0	1.56 m, 1.29 m	22.0	1.55 m, 1.31 m
12	41.3	2.01 dt (12.5, 3.0) 1.17 m	41.3	2.00 dt (12.4, 3.0) 1.16 m	41.3	1.99 dt (12.5, 3.0) 1.08 m
13	44.0		44.0		43.9	3.0
14	57.5	1.15 m	57.8	1.11 m	57.5	1.10 m
15	25.3	1.10 m, 1.57 m	25.3	1.10 m, 1.60 m	25.3	1.11 m, 1.61 m
16	29.4	1.36 m, 1.80 m	29.4	1.28 m, 1.90 m	29.4	1.31 m?, 1.84 m
17	57.8	1.15 m	57.7	1.11 m	57.8	1.10 m
18	12.6	0.69 s	12.6	0.69 s	12.6	0.68 s
19	15.5	1.06 s	15.5	1.06 s	15.5	1.06 s
20	37.9	1.35 m	37.8	1.35 m	38.0	1.28 m
21	19.7	0.95 d (6.7)	19.5	0.92 d (6.5)	19.4	0.90 d (6.5)
22	36.8	0.99 m, 1.86 m	34.6	1.06 m, 1.29 m	34.6	0.96 m, 1.38 m
23	29.3	0.85 m	34.5	1.35 m, 1.55 m	30.3	1.04 m, 1.49 m
24	45.5	1.03 m	24.9		29.0	
25	34.2		21.0		33.2	1.29 m
26	27.9	0.86 s	23.0	1.10 s	20.9	0.98 d (6.9)
27	27.9	0.86 s	23.3	1.07 s	20.9	1.01 d (6.9)
28	27.9	0.86 s	28.1	0.11 d (4.0) 0.06 d (4.0)	19.1	0.68 m
29	15.1	0.83 d (7.0)	20.1	1.05 s	20.4	–0.22 dd (5.5, 4.5) 0.44 dd (8.5, 4.5)
30	—	—	—	—	14.2	1.09 d (6.4)

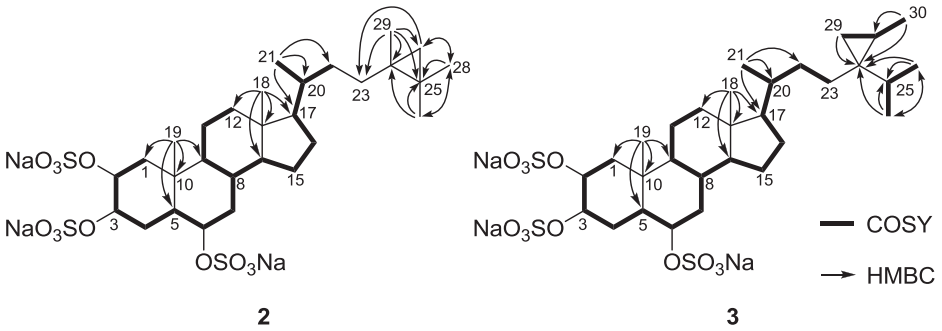

2 3

Figure 2 Key HMBC cross peaks of halistanol sulfates I (**2**) and J (**3**).

Table 2 SIRT1–3 inhibitory activity of compounds 1–3

	IC_{50} (μM)		
Compounds	*SIRT1 (± s.d.)*	*SIRT2 (± s.d.)*	*SIRT3 (± s.d.)*
Halistanol sulfate (**1**)	49.1 (1.7)	19.2 (0.68)	21.8 (0.36)
Halistanol sulfate I (**2**)	45.9 (3.9)	18.9 (0.59)	32.6 (2.13)
Halistanol sulfate J (**3**)	67.9 (4.7)	21.1 (0.82)	37.5 (3.70)
Nicotineamide (NA)	[a]	80.4 (4.3)	76.7 (13.9)

[a]Not tested.

deduced for **2**. The obvious differences between **1** and **2** lay in the terminal parts of the side chain; two down-field shifted doublets for methylene protons (δ_H 0.06 and 0.11) in **2**, instead of characteristic singlet methyl protons of *t*-butyl group at δ 0.86 in **1**, indicating that one of the methyl carbon directly bind to C-24 to form a cyclopropane ring. This terminal structure was secured by the HMBC cross peaks among H_3-29/C-23, C-24, C-25 and C-28, as well as H_3-26 and H_3-27/C-24, C-25 and C-28 (Figure 2). Although connectivity between C-22 and C-23 was not confirmed by COSY or HMBC analysis because of the ambiguous cross peaks caused by overlap of proton signals, the only possible structure fulfilling the molecular formula of **2** was as that shown in Figure 2. Comparison of ^1H (*J* value) and ^{13}C NMR signals of **2** with those of **1** indicated that the relative configuration of the steroidal part of **2** was the same as **1**, including 2*β*, 3*α*, 6*α*-hydroxy groups (δ_C 75.7, 75.7 and 78.9). The 20*R** configuration in **2** was also inferred by the chemical shift and the *J* value (δ_C 0.92 d, $J_H = 6.5$ Hz) of H-20. Although configuration of the same side chain was determined for the triterpene isolated from leaves of *Pandanus boninensis*,[12] we could only obtain the NMR data in $CDCl_3$. Therefore, we could not compare the NMR data of **2** that was not dissolved in $CDCl_3$, and as a result, the configuration at C-24 remains to be determined.

In the ESIMS of halistanol sulfate J (**3**), three characteristic sequential ion peaks were observed at *m/z* 743.3 $[M\text{-}Na]^-$, 623.3 $[743.3\text{-}NaSO_4H]^-$ and 503.3 $[623.3\text{-}NaSO_3H]^-$, indicating that compound **3** contains three sulfate groups as was the case for compound **2**. IR absorption at 1244 and 1220 cm^{-1} again supported the presence of sulfate groups. The molecular formula of compound **3** was determined as $C_{30}H_{49}Na_3O_{12}S_3$, which includes a CH_2 unit in addition to that of **2**, based on the HRESIMS analysis (*m/z* 743.2200 $[M\text{-}Na]^-$, calcd for $C_{30}H_{49}Na_2O_{12}S_3$ *m/z* 729.2187). ^1H and ^{13}C NMR spectra of **3** showed that it is also an analog of halistanol sulfate (**1**) bearing a cyclopropyl ring in the side chain (Table 1). ^1H-^1H COSY analysis revealed the presence of three spin systems (Figure 2). Along with HMQC and HMBC analysis, the core part (C-1 to C-23) was deduced to be identical to those of **1** and **2**. Different cyclization pattern and an additional more carbon on this ring were secured by HMBC cross peaks among H-29, H-30/C-24 and H-30/C-28. Attachment of an isopropyl group (C-25 to C-27) to C-24 was also confirmed by HMBC cross peaks among H-26 and H-27/C-24. Relative configuration of the core part was again assigned to be the same as that of **1** on the basis of superposition of their NMR data. Although the side chain structure of **3** was shared by weinbersterol disulfate B[13] and ibisterol sulfate,[9] the configuration at C-24 and C-28 was not determined for either compounds.

Halistanol sulfate (**1**) and halistanol sulfates I (**2**) and J (**3**) showed no cytotoxicity against HeLa and P388 cells at the concentration of 100 μM, while they showed SIRT1–3 inhibitory activities with IC_{50} values of 45.9–67.9, 18.9–21.1 and 21.8–37.5 μM, respectively (Table 2). However, halistanol sulfate (**1**) did not show the increase of the acetylation level of eIf5A, a physiological substrate of SIRT2 in the whole-cell assay.

Poly-sulfated steroids, including halistanol sulfate (**1**), are remarkable for their wide variety of bioactivities, such as antimicrobial, anti-HIV[14], and antifouling activities,[15] as well as enzyme inhibitory activities against protein kinases,[6] HIV reverse transcriptase,[16] HIV integrase,[17] glycosidases or proteases (unpublished data). However, inhibitory activities against KDACs or SIRTs have not yet been known. This is the first report of inhibitory activity of halistanol sulfates against SIRTs.

One of the possible mechanisms for the poly-sulfated steroids to interfere with the function of enzymes have been through the detergent-like nature of these type of compounds. However, the crystal structure of SIRT3–halistanol sulfate (**1**) complex (Figure 3) successfully obtained by sitting drop vapor diffusion method, suggests the possibility for a different mode of action of this compound (Table 3). The conformational change of the SIRT3 structure was shown to be induced by substrate binding.[18] In the crystal, two halistanol sulfate (**1**) molecules bind to one SIRT3 molecule (Figure 3). Two molecules of **1** are stacked through the steroid moieties on α-helix (Q300-M311) with hydrophobic surface formed by residues L303, L304, V306 and V307. Hydrogen bonding interactions are formed between sulfate ions of compound **1** and residues R224, K243, Q300 and R301. The binding sites are far from the active site H248, the substrate-binding sites or the co-factor NAD^+-binding site. The crystal structure suggests similar allosteric effects on antithrombin caused by heparin. Heparin, a sulfated polysaccharide, binding to the exosite of the molecule induces conformational change allowing complex formation with factor Xa.[19] Thus we found an allosteric site for SIRT3 inhibition, which is different from the resveratrol-binding allosteric sites.[20] This finding reveals the possibility that polysulfated steroids may mimic the binding mode to various

proteins by sulfated polysaccharides, such as heparin or haparan sulfate. Therefore, steroid sulfates can be a good motif to allosteric controller of enzymes.

MATERIALS AND METHODS

General experimental procedures

NMR spectra were recorded on Avance 400 MHz spectrometers (Bruker, Billerica, MA, USA). ^{1}H and ^{13}C NMR chemical shifts were referenced to the solvent peaks, δ_H 3.31 and δ_C 49.15 for CD_3OD. ESIMS were measured on a AccuTOF CS mass spectrometers (JEOL, Tokyo, Japan). HRESIMS were measured on a SCIENTIFIC Exactive Plus mass spectrometers (Thermo Fisher, Waltham, MA, USA). Optical rotation was determined on a JASCO DIP-1000 digital polarimeter in MeOH. UV spectra were recorded using a UV-1800 spectrophotometer (SHIMADZU Corporation, Kyoto, Japan). IR spectra were measured on a Nicolet 6700 spectrometer (Thermo Fisher, Waltham, MA, USA).

Table 3 Crystallographic statistics of SIRT3–halistanol sulfates (1)–AceCS2-K(Ac) peptide)

Data collection statistics			*Refinement statistics*	
X-ray source		PF BL17A	Resolution range (Å)	20.0–2.6
Space group		*P*432	No. of reflections	10 944
Unit cell	*a*, *b*, *c* (Å)	127.81	No. of non-hydrogen atoms	2166
	α, β, γ (°)	90.0	R_{work} (%)	22.5
Wavelength (Å)		0.980	R_{free} (%)	29.9
Resolution (Å)		50–2.6 (2.69–2.60)	R.m.s. deviations	
			Bond length (Å)	0.095
Unique reflections		11 529	Bond angle (degree)	1.572
Completeness (%)[a]		99.9	*B*-factors (Å^2)	
R_{merge} (%)[a]		6.4 (75.7)	Ramachandran plot (%)	
I/σ (%)[a]		88.8 (7.7)	Favored region	94.6
Wilson *B* (Å^2)		61.2	Allowed region	5.4
			Outlier region	0.0

[a]Values in parentheses are for the highest resolution shell.

Biological material

Halichondria sp. was collected by hand using SCUBA at the depth of 15 m, Sokodo, Hachijo-jima Island (N 33° 07.16', E 139° 49.07'), Tokyo, Japan in December 1994. The sample was immediately frozen and kept at −25 °C until extraction. The specimen was deposited in the Naturalis Biodiversity Center (RMNH POR 7354).

Isolation and identification

The sponge specimen (695 g w.w.) was extracted with MeOH (2 l×7) and the combined extract was evaporated *in vacuo*. The concentrated extract was suspended in H_2O and extracted with $CHCl_3$ and then *n*-BuOH. The $CHCl_3$ and *n*-BuOH layers were combined and subjected to the Kupchan procedure[21] yielding *n*-hexane, $CHCl_3$ and aqueous MeOH layers. The aqueous MeOH layer was concentrated to dryness and then separated by ODS flash chromatography (H_2O/MeOH = 100/0, 80/20, 50/50, 30/70 and 0/100 and $CHCl_3$/MeOH/H_2O = 6/4/1) to give six fractions (fr. A–F). Inhibitory activity against SIRT3 was found in the fraction eluting with H_2O/MeOH = 50/50 (fr. C). A part (500 mg) of this fr. C was further separated by the reversed-phase HPLC (column: COSMOSIL 5C_{18}-AR-II (250×20 mm^2), flow rate; 8 ml min^{-1}, detection; UV 220 nm and RI, solvent system: H_2O/MeOH = 25/75 with 200 mM $NaClO_4$) to yield 22 fractions (fr.1–22). Of these, fr.18 contained halistanol sulfate (**1**, 301.4 mg, 3.5×10^{-2}%, yield based on wet weight) and fr.9 contained 11.4 mg of crude halistanol sulfate I (**2**). Crude fr. 9 was purified by HPLC (column; COSMOSIL 5C_{18}-AR-II (250×10 mm^2), flow rate; 2 ml min^{-1}, detection; UV 220 nm and RI, solvent system; H_2O/MeOH = 20/80 with 200 mM $NaClO_4$) to afford pure compound **2** (6.6 mg, 9.5×10^{-3}%, yield based on wet weight).

Fr.22 contained crude halistanol sulfate J (**3**), which was purified by three-step reversed-phase HPLC; repetitive separation under the same condition (column: COSMOSIL 5C_{18}-AR-II (250×20 mm^2), flow rate; 8 ml min^{-1}, detection; UV 220 nm and RI, solvent system: H_2O/MeOH = 20/80 with 200 mM $NaClO_4$), followed by final purification under the different condition (column: COSMOSIL 5C_{18}-MS-II (250×10 mm^2), flow rate; 2 ml min^{-1}, detection; UV 220 nm and RI, solvent system: H_2O/MeOH = 25/75 with 200 mM $NaClO_4$), yielding 0.7 mg of halistanol sulfate J (**3**). To gain more amount of compound **3**, additional 560 mg of the fraction eluting with H_2O/MeOH = 50/50 (fr. C) was separated by HPLC (column: COSMOSIL 5C_{18}-AR-II (250×20 mm^2), flow rate; 8 ml min^{-1}, detection; UV 220 nm and RI, solvent system: H_2O/MeOH = 10/90 with 200 mM $NaClO_4$), followed by HPLC

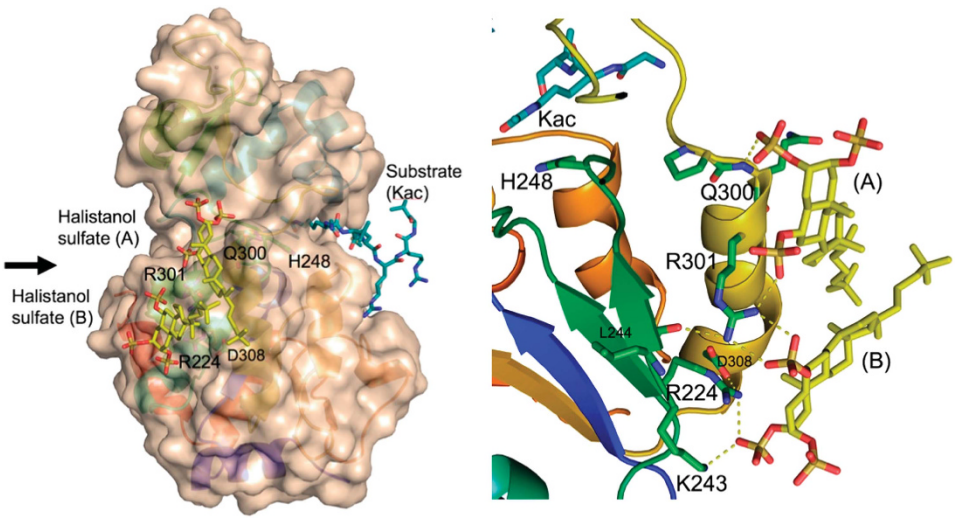

Figure 3 Crystal structure of SIRT3–halistanol sulfate (**1**) complex. (Left panel) Molecular surface of SIRT3 in complex with two halistanol sulfate (**1**) molecules and substrate acetyl lysine peptide. The arrow indicates the view point of the left panel. (Right panel) Close-up view of the halistanol sulfate-binding sites of SIRT3. Hydrogen bonding interactions are drawn in yellow dotted lines.

with the same column and with the different solvent system of H_2O/MeOH = 15/85 with 200 mM $NaClO_4$. Final purification was carried out by two-step recycling reversed-phase HPLC (column: COSMOSIL $5C_{18}$-MS-II (250×10 mm^2), flow rate; 2 ml min^{-1}, detection; UV 220 nm and RI, solvent system: H_2O/MeOH = 10/90 with 200 mM $NaClO_4$) to afford halistanol sulfate J (**3**, 3.0 mg, 5.5×10^{-3}%, yield based on wet weight).

*Halistanol sulfate (**1**).* Colorless amorphous solid; ESIMS *m/z* 731.3 $[M\text{-}Na]^-$, 611.3 $[M\text{-}Na\text{-}NaSO_4H]^-$, 509.4 $[M\text{-}Na\text{-}NaSO_4H\text{-}NaSO_3]^-$, 491.3 $[M\text{-}Na\text{-}2(NaSO_4H)]^-$, 354.1 $[M\text{-}2Na]^{2-}$; HRESIMS *m/z* 731.2194 $[M\text{-}Na]^-$ (calcd for $C_{29}H_{49}Na_2O_{12}S_3$ *m/z* 731.2187); for ^{1}H and ^{13}C NMR data, see Table 1.

*Halistanol sulfate I (**2**).* Colorless amorphous solid; $[\alpha]_D^{25.4}$ +25.0° (*c* 0.01, MeOH); UV (CH_3OH) λ_{max} (logε) 279(2.61) nm; IR (KBr) ν_{max} 2939, 2868, 1642, 1472, 1445, 1386, 1248, 1122, 1064, 968, 941, 930, 897, 826, 799, 754, 731, 628 cm^{-1}; ESIMS *m/z* 729.2 $[M\text{-}Na]^-$, 609.3 $[M\text{-}Na\text{-}NaSO_4H]^-$, 507.3 $[M\text{-}Na\text{-}NaSO_4H\text{-}NaSO_3]^-$, 489.3 $[M\text{-}Na\text{-}2(NaSO_4H)]^-$, 353.1 $[M\text{-}2Na]^{2-}$; HRESIMS analysis (*m/z* 729.2027 $[M\text{-}Na]^-$, calcd for $C_{29}H_{47}Na_2O_{12}S_3$ *m/z* 729.2031); for ^{1}H and ^{13}C NMR data, see Table 1.

*Halistanol sulfate J (**3**).* Colorless amorphous solid; $[\alpha]_D^{25.4}$ +32.0° (*c* 0.01, MeOH); UV (CH_3OH) λ_{max} (logε) 278 (2.67) nm; IR (KBr) ν_{max} 2934, 2870, 1633, 1472, 1454, 1382, 1244, 1126, 1972, 969, 930, 893, 844, 826, 799, 749, 732, 624 cm^{-1}; ESIMS *m/z* 743.3 $[M\text{-}Na]^-$, 623.3 $[M\text{-}Na\text{-}NaSO_4H]^-$, 521.4 $[M\text{-}Na\text{-}NaSO_4H\text{-}NaSO_3]^-$, 503.3 $[M\text{-}Na\text{-}2(NaSO_4H)]^-$, 360.1 $[M\text{-}2Na]^{2-}$; HRESIMS analysis (*m/z* 743.2200 $[M\text{-}Na]^-$, calcd for $C_{30}H_{49}Na_2O_{12}S_3$ *m/z* 729.2187); for ^{1}H and ^{13}C NMR data, see Table 1.

Cytotoxicity test

HeLa cells in Dulbecco's modified Eagle's medium (low glucose, Wako, Osaka, Japan), containing 10% of fetal bovine serum (Biosera, Ringmer, UK), 2 μg ml^{-1} of gentamicin reagent solution, 10 μg ml^{-1} of antibiotic–antimycotic were cultured at 37 °C under an atmosphere of 5% CO_2 with various concentrations of halistanol sulfates (**1**, **2** and **3**). P388 cells in RPMI-1640 medium (Wako), containing 10% of fetal bovine serum, HRDS solution (2, 2'-dithiobisethanol) and kanamycin sulfate were cultured at 37 °C under an atmosphere of 5% CO_2 with various concentrations of **1**, **2** and **3**. After 72 h cultivation, to each cell was added to 3-(4,5-dimethyl-2-thiazoyl)-2,5-diphenyl-2H tetrazolium bromide (MTT) saline solution and incubated. After 4 h, medium was removed by aspiration and dimethyl sulfoxide was added to lyse cells. Concentration of the reduced MTT was quantified by measuring the absorbance at 650 nm to estimate IC_{50} values.

SIRT inhibition assays

In vitro SIRT1–3 inhibitory tests were performed by an electrophoretic mobility shift assay as described previously.[22] Briefly, recombinant SIRT proteins were incubated with a carboxyfluorescein (FAM)-labeled acetylated lysine peptide (1.5 μM FAM-RHKK(Ac)LM for SIRT1 and SIRT2; 1.5 μM FAM-QPKK(Ac) KPL for SIRT3) and 1 mM NAD in 50 μl of assay buffer (25 mM Tris-HCl (pH 9.0), 137 mM NaCl, 2.7 mM KCl, 1 mM $MgCl_2$, 0.1 mg ml^{-1} bovine serum albumin) in 384-well plates for 60 min at 37 °C. After the reaction was stopped by adding in 50 μl of the stop buffer (100 mM HEPES (pH 7.5), 10 mM EDTA, 0.25% CR-3) containing nicotinamide (final concentration 10 mM), the samples were analyzed using a LabChip EZ Reader II (PerkinElmer, Waltham, MA, USA). Percentge of conversion is defined as $100 \times P/(P+S)$, where *P* and *S* are peak heights of product and peptide substrate, respectively.

Crystal structure of SIRT3 in complex with halistanol sulfate (1)

SIRT3 (residues:118–399, final concentration of 5 mg ml^{-1}), an acetylated lysine peptide (TRSGK(Ac)VMRRLLR: AceCS2-K(Ac), 1 mM) and halistanol sulfate (**1**, 1 mM) were mixed and crystallized. Crystals were obtained in 1.2 M sodium phosphate monobasic and potassium phosphate dibasic buffer, pH 5.4, at 20 °C, and frozen with liquid nitrogen, using 18% glycerol as a cryoprotectant. X-ray diffraction data were collected at 100 K in a nitrogen gas stream at the synchrotron beamlines, PF-AR NW12A and PF-17 A at Photon Factory, KEK. Data were processed and scaled with the HKL2000 program.[23] The crystal structures were determined by the molecular replacement method with MOLREP,[24] using the structure of SIRT3/AceCS2-K(Ac) complex[18] (PDB id 3GLU). Refinement and model building were performed with REFMAC5[25] and Coot.[26] The geometric quality of the model was assessed with MolProbity.[27] Data collection and refinement statistics are listed in Table 3. Structural illustrations were generated using PyMol (Schrödinger).

CONFLICT OF INTEREST

The authors declare no conflict of interest.

ACKNOWLEDGEMENTS

This paper is a part of the outcome of research performed under a Waseda University Grant-in-Aid for Scientific Research, the Strategic Research Platforms for Private University, a Matching Fund Subsidy from the Ministry of Education, Science, Sports, and Technology (MEXT), Japan, JSPS KAKENHI Grant Number 26221204 and the Project for Development of Innovative Research on Cancer Therapeutics (P-Direct). This work was inspired by the JSPS Asian Chemical Biology Initiative. This work was performed under the approval of the Photon Factory Program Advisory Committee (Proposal Nos. 2013G674 and 2015G615). Atomic coordinates and structural factors have been deposited in the Protein Data Bank (PDB id 3GLU).

DEDICATION

This work is dedicated to Professor K. C. Nicolaou celebrating his great scientific contribution to total synthesis of 27 highly complex and biologically important natural products.

1 Correia, M. *et al.* Sirtuins in metabolism, stemness and differentiation. *Biochim. Biophys. Acta* **1861**, 3444–3455 (2017).
2 Hall, J. A., Dominy, J. E., Lee, Y. & Puigserver, P. The sirtuin family's role in aging and age-associated pathologies. *J. Clin. Invest.* **123**, 973–979 (2013).
3 Narayan, N. *et al.* The NAD-dependent deacetylase SIRT2 is required for programmed necrosis. *Nature* **492**, 199–204 (2012).
4 Chopra, V. *et al.* The sirtuin 2 inhibitor AK-7 is neuroprotective in Huntington's disease mouse models. *Cell Rep.* **2**, 1492–1497 (2012).
5 Fusetani, N. & Matsunaga, S. Bioactive marine metabolites. II. Halistanol sulfate, an antimicrobial novel steroid sulfate from the marine sponge *Halichondria* cf. *moorei* Bergquist. *Tetrahedron Lett.* **22**, 1985–1988 (1981).
6 Slate, D., Lee, R. H., Rogoriguez, J. & Crews, P. The marine natural product, halistanol trisulfate, inhibits pp60$^{v\text{-}src}$ protein tyrosine kinase activity. *Biochem. Biophys. Res. Commun.* **203**, 260–264 (1994).
7 Lima, B. *et al.* Halistanol sulfate A and rodriguesines A and B are antimicrobial and antibiofilm agents against the cariogenic bacterium *Streptococcus mutans*. *Rev. Bras. Farmacogn.* **24**, 651–659 (2014).
8 Cardellina, J. H. II *et al.* A chemical screening strategy for the dereplication and prioritization of HIV-inhibitory aqueous natural products extracts. *J. Nat. Prod.* **56**, 1123–1129 (1993).
9 McKee, T. C., Cardellina, J. H. II, Tischler, M., Snader, K. M. & Boyd, M. R. Ibisterol sulfate, a novel HIV-inhibitory sulfated sterol from the deep water sponge *Topsentia* sp. *Tetrahedron Lett.* **34**, 389–392 (1993).
10 McKee, T. C. *et al.* HIV-inhibitory natural products. 11. Comparative studies of sulfated sterols from marine invertebrates. *J. Med. Chem.* **37**, 793–797 (1994).
11 Nakao, Y. & Fusetani, N. Enzyme inhibitors from marine invertebrates. *J. Nat. Prod.* **70**, 689–710 (2007).
12 Inada, A. *et al.* Unusual cyclolanostanes from leaves of *Pandanus boninensis*. *Phytochemistry* **66**, 2729–2733 (2005).
13 Sun, H. H., Cross, S. S., Gunasekera, M. & Koehn, F. E. Weinbersterol disulfates A and B, antiviral steroid sulfates from the sponge *Petrosia weinbergi*. *Tetrahedron* **47**, 1185–1190 (1991).
14 Bifulco, G., Bruno, I., Minale, L. & Riccio, R. Novel HIV-inhibitory halistanol sulfates F-H from a marine sponge *Pseudoaxinissa digitata*. *J. Nat. Prod.* **57**, 164–167 (1994).
15 Tsukamoto, S., Kato, H., Hirota, H. & Fusetani, N. Antifouling terpenes and steroids against barnacle larvae from marine sponges. *Biofouling* **11**, 283–291 (1997).
16 Rudi, A. *et al.* Clathsterol, a novel anti-HIV-1 RTase sulphated sterol from the sponge *Clathria* species. *J. Nat. Prod.* **64**, 1451–1453 (2001).
17 Queresi, A & Faulkner, D. J Haplosamates A and B: new steroidal sulfamate esters from two haplosclerida sponges. *Tetrahedron* **55**, 8323–8330 (1999).
18 Jin, L. *et al.* Crystal structures of human SIRT3 displaying substrate-induced conformational changes. *J. Biol. Chem.* **284**, 24394–24405 (2009).
19 Jin, L. *et al.* The anticoagulant activation of antithrombin by heparin. *Proc. Natl Acad. Sci. USA* **94**, 14683–14688 (1997).
20 Nguyen, G. T. T., Gertz, M. & Steegborn, C. Crystal structures of Sirt3 complexes with 4'-bromo-resveratrol reveal binding sites and inhibition mechanism. *Chem. Biol.* **20**, 1375–1385 (2013).

21 Kupchan, S. M., Briton, R. W., Ziegler, M. F. & Sigel, C. W. Bruceantin, a new potent antileukemic simaroubolide from *Brucea antidysenterica*. *J. Org. Chem.* **38**, 178–179 (1973).
22 Shah, A. A., Ito, A., Nakata, A. & Yoshida, M. Identification of a selective SIRT2 inhibitor and its anti-breast cancer activity. *Biol. Pharm. Bull.* **39**, 1739–1742 (2016).
23 Otwinowski, Z. & Minor, W. Processing of X-ray diffraction data collected in oscillation mode. *Macromol. Crystallogr. A* **276**, 307–326 (1997).
24 Vagin, A. & Teplyakov, A. MOLREP: an automated program for molecular replacement. *J. Appl. Cryst.* **30**, 1022–1025 (1997).
25 Murshudov, G. N., Vagin, A. A. & Dodson, E. J. Refinement of macromolecular structures by the maximum-likelihood method. *Acta Crystallogr. D Biol. Crystallogr.* **53**, 240–255 (1997).
26 Emsley, P., Lohkamp, B., Scott, W. G. & Cowtan, K. Features and development of Coot. *Acta Crystallogr. D Biol. Crystallogr.* **66**, 486–501 (2010).
27 Chen, V. B. *et al.* MolProbity: all-atom structure validation for macromolecular crystallography. *Acta Crystallogr. D Biol. Crystallogr.* **66**, 12–21 (2010).

Supplementary Information accompanies the paper on The Journal of Antibiotics website (http://www.nature.com/ja)